Korean J. Chem. Eng., **16**(4), 482-488 (1999)

Numerical Simulation of Industrial Boilers

F. McKenty†, L. Gravel and R. Camarero

Centre Recherche en Calcul Appliqué (CERCA), 5160 boul. Décarie, bureau 400, Montréal, PQ, H3X 2H9, Canada
(*Received 15 December 1998 • accepted 26 April 1999*)

Abstract–The numerical simulation of combustion aerodynamics is a topic that has been generating much interest in the past few years. Much research has been devoted to this field since the late 1960's, and many models of varying complexity were developed. However, most of the computational effort was devoted to the validation of these various models on experimental geometries. Furthermore, most of these models were only available within the framework of research codes : commercial CFD software offered only the most basic of models to their users. In recent years, with the advent of more powerful and affordable workstations, the feasibility of treating very large coupled problems became a reality. Consequently, the incentive for commercial CFD code developers to apply their product to the simulation of industrial combustion phenomena brought about a lot of activity in this field. The result was the possibility to include sophisticated modelling of this complex physical phenomena within the framework of commercial codes designed to solve flows in very large and complex geometries. This presentation will endeavour to show that by interfacing a commercial CFD package (Star-CD) with a research combustion model library we were able to successfully simulate several different types of industrial boilers and incinerators fired with different types of fuels (gas, oil, wood). Though precise measurements inside industrial boilers are difficult to obtain, comparisons with measurements taken at the various outlets show good agreement with the predicted values. Furthermore, the simulations predicted trouble spots within the apparatus that were in close agreement with the manufacturer's field observations. In short, the numerical simulation of industrial combustion is not only qualitative, in the sense that it can correctly predict trends, but is well on its way to being quantitatively correct.

Key words : CFD, Combustion, Boilers, NO_x, Burners

INTRODUCTION

Combustion in industrial boilers, ovens and incinerators can be quite difficult to simulate because it involves several closely coupled complex physical phenomena. The first and most obvious of these is the solution of highly turbulent flow, mixing and mass transfer within large enclosures. Additionally, one must then consider the chemical reactions themselves which being exothermic are accompanied by intense heat transfer. This heat transfer is of course convective, but is often also highly radiative. Finally, many components of the flue gases are environmental pollutants and the emmission levels are of great interest to manufacturers and operators alike.

In the past, burner and boiler designs were largely based on empirical laws and on past experience. However, with advent of much stricter norms and regulations on emission levels and with the rising cost of fossil fuels, these tried and tested methods of design are no longer adequate to meet the demand for more efficient and environmentally friendly combustion apparatus. The main difficulty resides in knowing what is truly happening inside the enclosure : manufacturers have the know-how to solve most combustion problems, but these must first be identified. It is already quite expensive and laborious to properly instrument an experimental combustor designed for that purpose, the task becomes close to impossible when dealing with large industrial apparatus. Consequently, it is very difficult for an engineer to get a clear picture of what is going on. To be able to optimise the design, the engineer requires information that is unavailable through conventional means (description of the flow field, temperature and chemical species distributions). In short, the enclosure constitutes a black box where there is no accurate knowledge of how these different physical phenomena are interacting. Because of all these unknown variables, the burners must often be adjusted in the field in order to meet emmission levels (if possible). This action most often results in a loss of efficiency since the unit is no longer operating at nominal design conditions. The problem is compounded by the fact that flame aerodynamics are influenced as much by the enclosure geometry as by the burner geometry itself. Which is to say that a particular burner design operating satisfactorily in one boiler could have a pitiful performance in another boiler geometry. Therefore, one cannot hope to devise a perfect burner design for one application and easily transfer the technology to another. Analysis must be made on an almost case by case basis.

The modelling of combustion phenomena is now sufficiently mature to be applied to industrial cases with confidence. These models coupled with the capacity of commercial CFD software such as Star-CD to efficiently solve very large problems in a relatively short time frame, has made full numerical simulation of industrial combustion apparatus a reality. Hence, the engineer can easily evaluate his design and the impact of modifications to that design prior to construction. Not only will this tool enable the engineer to gain greater understanding of the phenomena at hand and allow for better designs, it will significantly reduce manufactur-

†To whom correspondence should be addressed.
E-mail : mckenty@cerca.umontreal.ca

ing costs in the long run. Furthermore, it is quite conceivable that within a decade most combustion apparatus design will be done through CFD just as it is now the norm within the aeronautics industry. Manufacturers who fail to jump on the bandwagon may well be left out in the cold.

GOVERNING EQUATIONS

Unsteady, turbulent mean flows for a weakly compressible fluid are governed by the following Favre averaged equations for mass conservation, momentum transport and scalar transport.

$$\frac{\partial\bar{\rho}}{\partial t}+\nabla\cdot(\bar{\rho}\tilde{\mathbf{U}})=0 \tag{1}$$

$$\frac{\partial}{\partial t}(\bar{\rho}\tilde{\mathbf{U}})+\nabla\cdot[\bar{\rho}\tilde{\mathbf{U}}\otimes\tilde{\mathbf{U}}-\mu_{eff}(\nabla\tilde{\mathbf{U}}+\nabla^{T}\tilde{\mathbf{U}})]=-\nabla\cdot(\bar{p}\tilde{\mathbf{G}})+\tilde{\mathbf{S}}_{i} \tag{2}$$

$$\frac{\partial}{\partial t}(\bar{\rho}\tilde{\phi})+\nabla\cdot[\bar{\rho}\tilde{\mathbf{U}}\tilde{\phi}-\Gamma_{\phi}\nabla\tilde{\phi}]=\tilde{S}_{\phi} \tag{3}$$

where $\otimes$ is the tensor product operator, $\tilde{\tilde{\mathbf{G}}}$ is the metric tensor, Γ_{ϕ} is the diffusion coefficient and S is a source term. The effective viscosity, μ_{eff} is defined by :

$$\mu_{eff}=\mu+\mu_{t} \tag{4}$$

where μ is the laminar viscosity and μ_t is the eddy viscosity that can be written in the case of the standard k–ε turbulence model as :

$$\mu_{t}=C_{\mu}\bar{\rho}\frac{\bar{k}^{2}}{\varepsilon} \tag{5}$$

This formulation is completed by solving the transport equations that express the conservation of the turbulent kinetic energy κ and its dissipation rate ε :

$$\frac{\partial}{\partial t}(\bar{\rho}k)+\nabla\cdot\left[\bar{\rho}\tilde{\mathbf{U}}k-\left(\mu+\frac{\mu t}{\sigma_{k}}\right)\nabla k\right]=P_{k}-\bar{\rho}\varepsilon \tag{6}$$

$$\frac{\partial}{\partial t}(\bar{\rho}\varepsilon)+\nabla\cdot\left[\bar{\rho}\tilde{\mathbf{U}}\varepsilon-\left(\mu+\frac{\mu t}{\sigma_{\varepsilon}}\right)\nabla\varepsilon\right]=(C_{\varepsilon 1}P_{k}-C_{\varepsilon 2}\bar{\rho}\varepsilon)\frac{\varepsilon}{k} \tag{7}$$

where P_k represents the production of turbulent kinetic energy and is given by :

$$P_{k}=2\mu_{t}\mathrm{tr}(\tilde{\tilde{\mathbf{D}}}\tilde{\tilde{\mathbf{D}}})=2\mu_{t}D_{ij}D_{ij} \tag{8}$$

where $\tilde{\tilde{\mathbf{D}}}$ is the strength rate tensor and tr(.) is the trace operator. The k–ε model has five closure coefficients that are determined by replacing double and triple correlations with algebraic expressions involving known turbulence and mean flow properties [Launder and Spalding, 1974]. The following common values are used :

σ_k	σ_ε	$C_{\varepsilon 1}$	$C_{\varepsilon 2}$	C_μ
1.0	1.3	1.44	1.92	0.09

COMBUSTION MODELLING

The major difficulty in modelling turbulent flames is the determination of the turbulent reaction rate for the various chemical species [i.e. the source term in Eq. (3)]. Instantaneous chemical reaction rates are commonly give by the Arrhenius relation :

$$R_{fuel}=k_{s}\rho^{2}m_{fuel}m_{O_2} \tag{9}$$

with

$$k_{s}=Ae^{-E/(RT)} \tag{10}$$

where A is the frequency or pre-exponential factor and E is the activation energy. Unfortunately, for turbulent mean flow calculations, an instantaneous value must be expressed in terms of mean value and its turbulent fluctuation. Using Reynolds averaging, this may be expressed as :

$$\phi_{instantaneous}=\bar{\phi}_{average}+\phi'_{fluctuation} \tag{11}$$

Consequently, the mean reaction rate must then be expressed as :

$$\bar{R}_{fuel}=(\bar{k}_{s}+k'_{s})(\bar{\rho}+\rho')^{2}(\bar{m}_{fuel}+m'_{fuel})(\bar{m}_{O_2}+m'_{O_2}) \tag{12}$$

and therefore the mean reactioin rate is not equal to the reaction rate based on mean values. In fact, when the products in the previous equation are carried out the following expression is found :

$$\bar{R}_{fuel}=A\bar{\rho}^{2}\bar{m}_{fuel}\bar{m}_{O_2}e^{-E/RT}(1+\Upsilon) \tag{13}$$

$$\Upsilon=a_{0}\frac{\overline{m'_{fuel}\,m'_{O_2}}}{\bar{m}_{fuel}\bar{m}_{O_2}}+a_{1}\frac{\overline{T'^{2}}}{\bar{T}^{2}}+a_{2}\left(\frac{\overline{T'm'_{fuel}}}{\bar{T}\bar{m}_{fuel}}+\frac{\overline{T'm'_{O_2}}}{\bar{T}\bar{m}_{O_2}}\right) \tag{14}$$

with

$$a_{0}=1 \quad a_{1}=\frac{1}{2}\left(\frac{E}{R\bar{T}}\right)^{2}-\frac{E}{R\bar{T}} \quad a_{2}=\frac{E}{R\bar{T}} \tag{15}$$

where the Υ term contains several second order correlations for turbulent fluctuations. Taking these second order correlations into account would require an additional transport equation per correlation. Furthermore, all these second order correlations are functions of higher order correlations which are also unknown. This constitutes a perpetual closure problem for the system of equations that cannot be easily resolved. Failure to take the turbulent correlations of the Υ term into accoutnt could result in serious error for the reaction rate [Khalil, 1982]. Taking these correlations into account would be very complex and much too expensive a venture in the context of industrial size simulations where the calculation domains are regularly made up of at least a million computational cells.

Fortunately, for non-premixed flames, the time scale of the reaction rate is very small compared to the time scale for turbulent mixing of the fuel and oxidant. Therefore, the turbulent mixing rate can be considered to control the overall reaction rate (i.e. the reactants cannot react until they actually meet). Consequently, the chemical reaction itself may be considered to be very fast compared to the mixing process. This enables the formulation of what is called the "diffusion flame hypothesis" where chemical reactions are considered to be so fast compared to the mixing process that chemical equilibrium is assumed to be reached locally (within a computational cell) within the mixture's residence time at the prevailing local conditions. However, it must be emphasized that this is only a model and this hypothesis breaks down for fuel rich mixtures. This shortcoming can be greatly reduced by considering the flame to be made up of pockets of unburnt fuel and oxidant separated by thin laminar flamelets which are influenced

by the turbulent flow. It is thus possible to construct a laminar flamelet library based on experimental data obtained from laminar flames. This last approach yields much better results in fuel rich regions, however it is limited to the availability of experimental laminar flame data for the fuel in question.

Whichever approach is used, the diffusion flame hypothesis has the additional advantage of allowing the concentrations of reacted chemical species to be determined as a function of the initial reactant concentrations. These in turn can be determined from the transport of a single non-dimensional conserved scalar f called mixture fraction which is defined as follows by supposing equal diffusion coefficients for all species (i.e. the turbulent Schmidt number is equal for all species) :

$$f=\frac{\zeta-\zeta_A}{\zeta_F-\zeta_A} \tag{16}$$

where

$$\zeta=m_{fuel}-\frac{m_{O_2}}{s} \tag{17}$$

The local reactant concentrations are then determined from the mean mixture fraction transport equation :

$$\frac{\partial}{\partial t}(\bar{\rho}\tilde{f})+\nabla\cdot\left[\bar{\rho}\tilde{\mathbf{U}}\tilde{f}-\left(\mu+\frac{\mu_t}{\sigma_f}\right)\nabla\tilde{f}\right]=0 \tag{18}$$

where $\tilde{f}=0$ represents pure oxidant, $\tilde{f}=1$ pure fuel and $0<\tilde{f}<1$ a particular mixture of fuel and oxidant. Consequently, all reacted species concentrations can now be expressed solely as a function of $\tilde{f}$.

Finally, the influence of turbulent fluctuations on the chemical reaction is introduced through an averaging process using probability density functions (PDF). The mean value of any chemical species ϕ which is a function of mixture fraction may be expressed as :

$$\tilde{\phi}=\int_0^1\phi(f)P(f)df \tag{19}$$

where P(f) is a beta probability density function determined as a function of the mean mixture fraction $\tilde{f}$ and of its variance $g=\tilde{f}''^2$

$$P(f)=\frac{f^{a-1}(1-f)^{b-1}}{\int_0^1 f^{a-1}(1-f)^{b-1}df} \tag{20}$$

where

$$a=\tilde{f}\left(\frac{\tilde{f}(1-\tilde{f})}{g}-1\right) \qquad b=\frac{(1-\tilde{f})}{\tilde{f}}a$$

Values for turbulent mixture fraction fluctuations are obtained from the solution of the transport equation for g where C_{g1} and C_{g2} are model constants [Khalil, 1982] :

$$\nabla\cdot(\bar{\rho}\tilde{\mathbf{U}}g-\Gamma_g\nabla g)=C_{g1}\mu_{eff}+(\nabla\tilde{f})^2-C_{g2}\bar{\rho}\frac{\varepsilon}{k}g \tag{21}$$

There are also other approaches to modelling turbulent non-premixed flame reaction rates. The most commonly employed of these is the Eddy-Breakup Model [Spalding, 1971; Hjertagger and Magnussen, 1982]. However, this class of model is highly dependant on the value of certain arbitrary constants which are flow dependant (i.e. the same value for the model's constants cannot be used for all types of flows and must be "tuned" according to the problem at hand in order to obtain satisfactory results). This class of model is therefore considered ill-suited for general industrial boiler simulations.

More detailed information on the combustion models used in this study may be found in [McKenty, 1992; Meng, 1994; Perrin et al., 1996; Rida, 1998].

INDUSTRIAL BOILER SIMULATIONS

CERCA has carried out the numerical simulation of seven different types of industrial boilers ranging in power from 30 MW to 286 MW. These boilers were fired with either natural gas, oil or wood bark. The number of burners installed on each boiler ranged from one to nine. In each case, the complete burner geometry was discretised. This is absolutely necessary if the correct flame dynamics are to be predicted. All simulations were carried out using the STAR-CD fluid dynamics code equipped with an interface allowing CERCA to input its own combustion model library to handle the reactive part of the problem. The natural gas fired boilers were simulated using CERCA's micro-flame model (laminar flamelet model) which yielded excellent results. The oil fired boiler was simulated using Star-CD's lagrangian particle tracking model for oil droplet vaporisation coupled to CERCA's constrained chemical equilibrium model. Finally the wood bark fired recovery boiler was simulated using a wood bark pyrolysis model coupled with CERCA's constrained chemical equilibrium model. Pollutant formation such as nitric oxide formation was simulated using CERCA's own models. All other models used to simulate other aspects of the flow (turbulence, heat transfer, lagrangian particle tracking, participating medium radiation etc...) were standard STAR-CD issue and performed very well.

These simulations were carried out on relatively small workstations (IBM 595 : 250 MFLOPS, 1 Gb RAM) so mesh size was a crucial consideration. Most meshes comprised between 500,000 and 900,000 computational cells which was considered the very minimum in order to obtain reliable predictions. Ideally, the meshes should contain at least 5 million computational cells in order to be assured the solution is not mesh dependant. At this point, we should point out that the limiting factor in this case was the available RAM on the workstation and not the STAR-CD software which can easily accommodate meshes larger than 10 million cells.

The computational mesh is of crucial importance for this type of analysis : it must be fine enough to allow for adequate resolution of burner aerodynamics. Lately, several articles have been published in trade journals claiming full boiler simulations with 70,000 computational cells. However, in order to accurately capture the mixing phenomena, we have found that for a typical industrial parallel flow gas burner, a minimum of 60,000 to 80,000 cells are necessary to discretise the area of the burner quarl alone. Therefore, we find it difficult to consider the results of full boiler simulations car-

ried out with less than half a million computational cells as anything but a very rough approximation.

RESULTS

Due to the limited space available for this paper, it will not be possible to present all the colour contour maps that constitute the detailed simulation results and that are crucial to understanding the analysis. These will be presented at the workshop. Nevertheless, we will endeavour to give the reader a general idea of what can be achieved using numerical simulation as a design tool for the optimisation of industrial combustion apparatus.

There are very few measurements available to validate the numerical predictions for full boiler simulations. The few measurements available were made in the field by the manufacturer. However, the CFD code and the combustion models were extensively and successfully validated on experimental combustors [McKenty, 1992; Meng, 1994; Gravel, 1994; Perrin et al., 1996; Rida, 1998]. The following comparisons are by no means extensive, but show that predictions agree quite closely with the few available measurements. Furthermore, the simulations agreed qualitatively with field observations in terms of flame length and shape as well as with observed throuble spots inside the furnace area (hot spots, tube-fouling etc...).

1. D-Type Boiler

The first type of boiler to be analysed is a 30 MW D-type boiler. The mesh for this boiler comprised 590,000 computational cells (Fig. 1). This boiler is fired with a natural gas parallel flow burner (Fig. 2). Approximately 60,000 computational cells were required for discretization of the burner quarl. For memory considerations, it is impossible to discretise every tube in the tube banks. Nevertheless, it is vital to include this equipment in the simulations as they constitute an non-negligible restriction to the fluid flow. Thus, the tube banks were modelled using head loss, and heat loss sink terms in the momentum and enthalpy equations respectively. The respective sink terms were determined by carrying out a full 3D simulation of small, but representative, portions of the tube banks and devising correlations from the numerical results. In short, we used the CFD code as a numerical test bed.

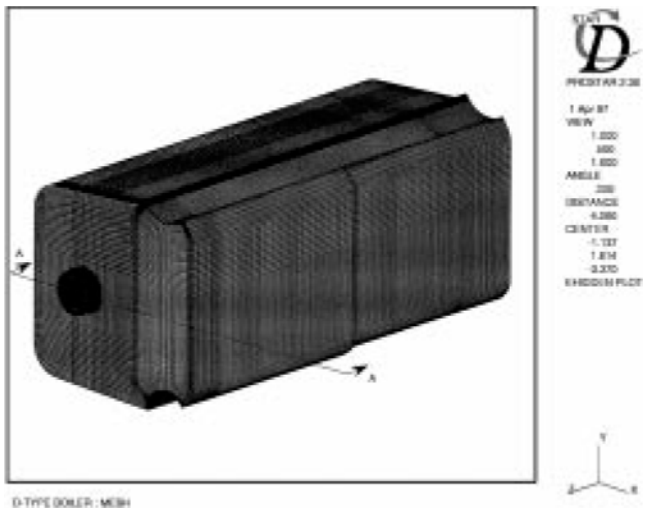

Fig. 1. D-Type Boiler : Computational mesh.

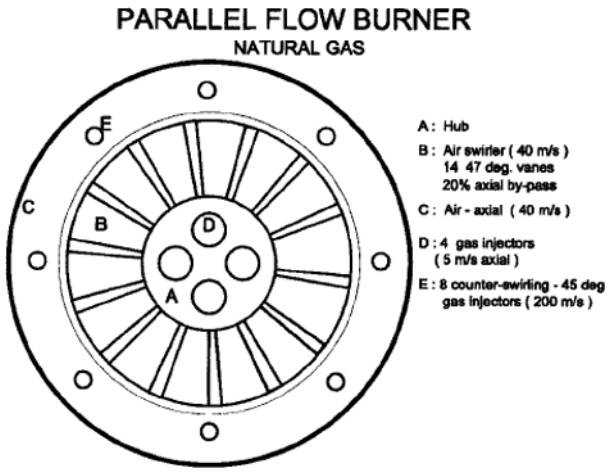

Fig. 2. D-Type Boiler : Computational mesh.

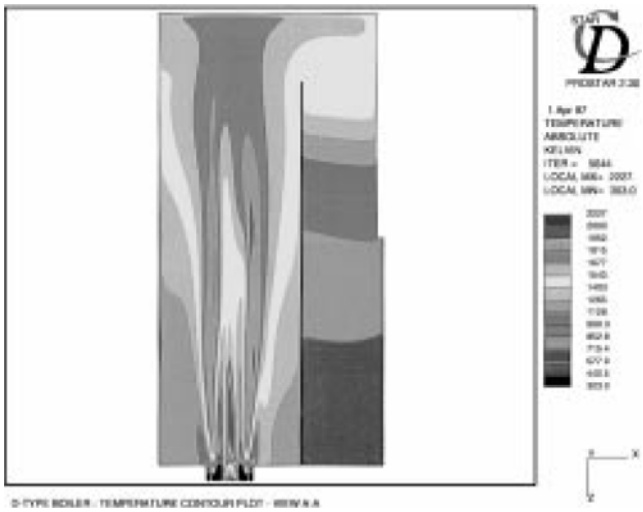

Fig. 3. D-Type Boiler : Temperature contour plothorizontal plane.

Fig. 3 shows a temperature contour plot in the boiler horizontal plane. The flame can be seen to be asymmetrical : this is due to the lack of symmetry of the furnace area of this boiler. The mean furnace outlet temperature predictions of 1,423 K compared very well with the measured field value of 1,445 K : an error of 1.5 %. Mean temperatures of the tube bank midsection also compared favourably : 858 K predicted vs 814 K measured or a relative error of 5.4 %. At the tube bank exit mean predicted temperature was of 596 K compared to a measured value of 570 K for a relative error of 4.6 %.

Predicted head losses in the tube banks were 1,012 Pa compared to measured values of 1,148 Pa, or a relative error of 11.8 %.

Fig. 4 shows a NO_x contour plot in the horizontal plane for the D-Type boiler. The predicted NO_x emission levels at furnace exit were of 120 ppm which compared favourably with 128 ppm value measured by boiler the manufacturer.

2. A-Type Boiler

The second boiler to be analysed is a 47 MW A-Type boiler. The mesh for this boiler comprised 400,000 computational cells (Fig.

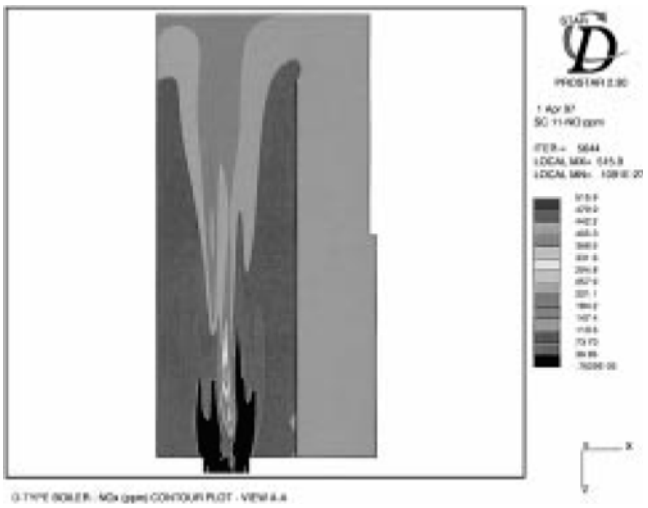

Fig. 4. D-Type Boiler : NO_x concentration contour plot-horizontal plane.

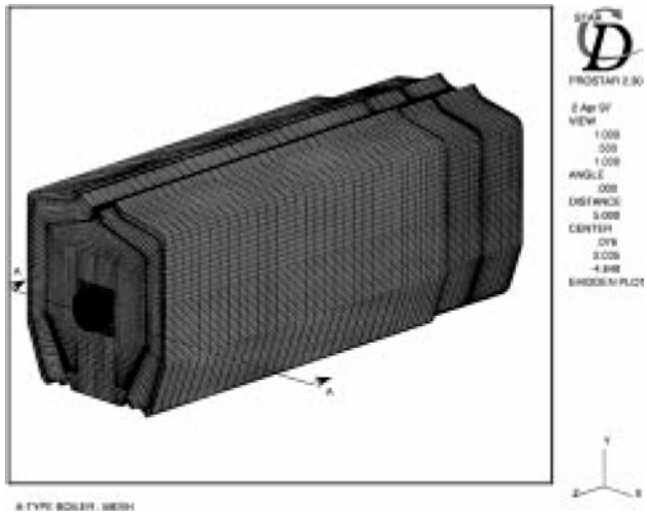

Fig. 5. A-Type Boiler : Computational mesh.

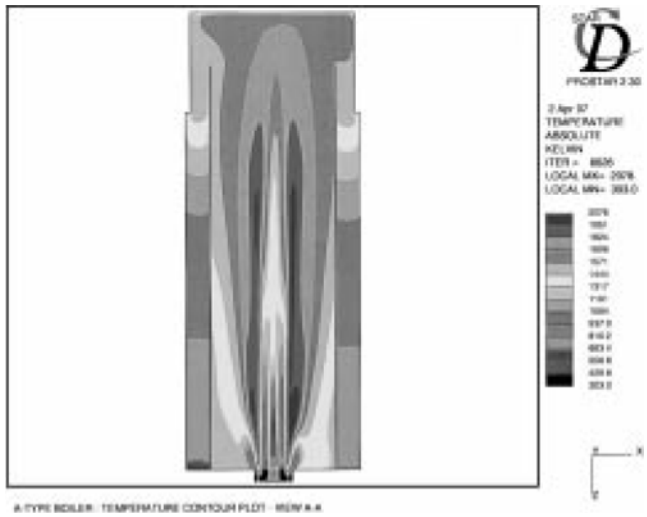

Fig. 6. A-Type Boiler : Temperature contour plot-horizontal plane.

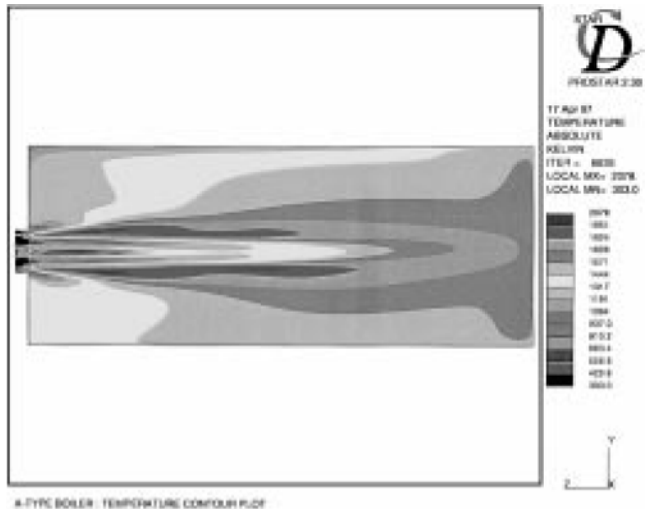

Fig. 7. A-Type Boiler : Temperature contour plot-vertical plane.

5). This boiler is also fired with natural gas and the same parallel flow burner design as for the D-type boiler was used.

Fig. 6 shows a temperature contour plot in the boiler horizontal plane and Fig. 7 shows a temperature contour plot in the boiler vertical plane. For this boiler the flame is symmetrical in the horizontal plane, but asymmetrical in the vertical plane thus demonstrating the influence of the enclosure geometry on flame aerodynamics. The predicted mean furnace outlet temperature of 1,451 K compared well with the measured value of 1,497 K, an error of 3.1 %. At the tube bank exit predicted mean temperature values and measured values are virtually identical at 621 K.

Predicted head losses in the tube banks were 690 Pa compared to measured values of 686 Pa, or a relative error of 0.5 %.

Fig. 8 shows the NO_x contour plot in the horizontal plane for the A-Type boiler. No NO_x concentration measurements were available for this boiler, but Fig. 8 is included here as it is interesting to note that the area of maximum NO_x for mation for the

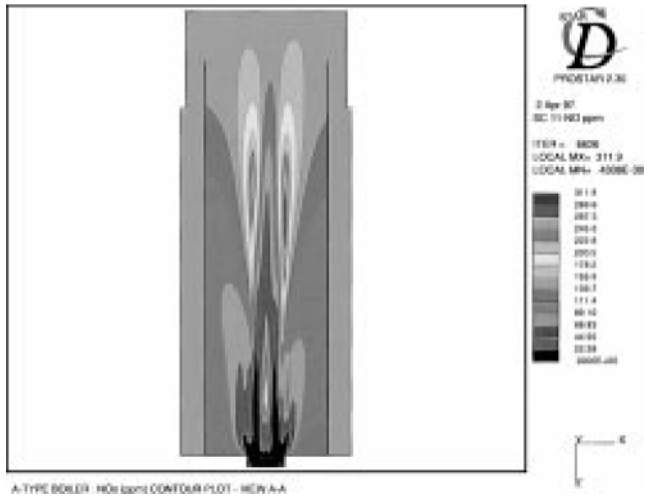

Fig. 8. A-Type Boiler : NO_x concentration contour plot-horizontal plane.

A-Type boiler is much further aft in this boiler than in the previous example.

DISCUSSION

Although very few experimental values taken on industrial boilers are available for validation purposes, the values we do have concur very well with the numerical predictions. In fact, for most cases, the error between measured and predicted values falls well within the boundaries of experimental error for all of the seven cases studied. We are by no means saying that all simulation results are quantitatively correct, however the excellent agreement with the available measurements suggests that these simulations are much more than only qualitative. Moreover, in light of these results, the engineer can most certainly use this tool in a very efficient manner to correctly predict trends and modify design parameters accordingly.

As a simple example of how numerical simulation gives greater insight to the designer and allows for better comprehension of the physical phenomena, let us consider the case of NO_x formation. Simply put, thermal NO_x formation requires the simultaneous presence of high temperature (T>1,800 K) and sufficient concentrations of oxygen and nitrogen. One would expect that, for a given burner design, the regions where these conditions are met are invariant. However, Figs. 4 and 8 show that this is effectively not the case : regions of high NO_x production are very different from one boiler to the other. This is because flame aerodynamics are as much a function of the geometry of the enclosure as of the burner itself : they are undissociable. It is quite obvious that this is the case when examining Figs. 3 and 6 as well as Figs. 4 and 8. It is also quite obvious that these results could not have been foreseen *a priori* : the burner-boiler design engineer could not have imagined this behaviour and could not have predicted it either without numerical simulations. However, having identified a potential problem, the engineer can then imagine design solutions to remedy the problem. Then, it is also a relatively simple task to verify if the devised solution is acceptable. Thus, the design process is still one of trial and error with the appreciable difference of not having to actually build the apparatus in order to verify the assumptions. The design process thus becomes more precise, faster and very cost effective.

CONCLUSION

The numerical simulation of combustion phenomena has been successfully applied in seven different types of industrial boilers. Though relatively few, comparisons between predicted and measured values are excellent. This technology is now sufficiently mature for it to be applied with confidence by boiler-burner design engineers in order to optimise their product and thus meet the demands and expectations of their customers. However, one must keep in mind that in order to accurately capture the extremely complex coupled physical phenomena involved, the numerical simulation of industrial phenomena cannot be approached in a haphazard fashion. Care must be taken to ensure that the computational grid offers sufficient resolution so that the results are not mesh dependant.

ACKNOWLEDGEMENTS

The authors wish to acknowledge Adapco/Star-CD for their participation and help in making the successful completion of this project possible.

NOMENCLATURE

A : frequency factor
C_{gi} : source term constants in g transport equation
$C_{\varepsilon i}$: constants; closure coefficients of the k–ε model
C_{μ} : constant; closure coefficient of the k–ε model
D : strength rate tensor
E : energy of activation
f : mixture fraction
g : turbulent mixture fraction fluctuation
k : turbulent kinetic energy
k_r : reaction rate constant
m : mass fraction
P_k : production of turbulent kinetic energy
P(f) : probability density function
R : universal gas constant
R_{fuel} : reaction rate
S_ϕ : source term in transport equation of ϕ
s : stoichiometric reaction coefficient
T : temperature
t : time
U : velocity vector

Greek Letters

Γ_ϕ : diffusion coefficient of scalar ϕ
ε : dissipation rate of turbulent kinetic energy
μ : laminar viscosity
μ_{eff} : effective viscosity
μ_t : turbulent viscosity
ρ : density
σ_ϕ : turbulent Prandtl or Schmidt number
ϕ : scalar

Symbols

tr : trace operator
∇ : nabla operator
- : mean value; Reynolds averaging
~ : mean value; Favre averaging
' : fluctuation; Reynolds averaging
" : fluctuation; Favre averaging
$\otimes$: tensor product

REFERENCES

Gravel, L., "Analyse paramétrique et optimisation d'un code de simulation numérique pour les phénomènes de combustion," Master's thesis, École Polytechnique de Montréal, Canada (1994).
Hjertagger, B. H. and Magnussen, B. F., "Computer Simulation

of Flow, Heat Transfer and Combustion of Three-Dimensional Furnaces," *Arch. Combus.*, **2**(1-2), 25 (1982).

Khalil, E. E., "Modelling of Furnaces and Combustors," Abacus Press, Tunbridge Well, UK (1982).

Launder, B. E. and Spalding, D. B., "The Numerical Computation of Turbulent Flows," *Comput. Meth. in Appl. Mech. Eng.*, **3**, 269 (1974).

McKenty, F., "Modèles de combustion pour la simulation numérique d'écoulements réactifs en atmosphère confinée," PhD thesis, École Polytechnique de Montréal, Canada (1992).

Meng, F. L., "A Staggered Control Volume Finite Element Method for Turbulent Reacting Flows Coupled with Radiation," PhD thesis, École Polytechnique de Montréal, Canada (1994).

Perrin, M., McKenty, F., Rida, S. and Camarero, R., "Experimental and Numerical Investigation of Natural Gas Non-premixed Turbulent Flames of Industrial Scale," In Combustion Canada 96 Conference, Ottawa, Canada (1994).

Rida, S., "Modélisation des Phénomènes de Combustion Pour la Simulation Numérique d'Écoulements Turbulents Réactifs," PhD thesis, École Polytechnique de Montréal, Canada (1998).

Spalding, D. B., "Mixing and Chemical Reaction in Steady Confined Turbulent Flames," In Thirteenth Symposium (Intl) on Combusion, 649 (1971).